Optimization of a FBG-based filtering module for a 40 Gb/s OSSB transmission system

Miguel V. DRUMMOND[1*], Artur FERREIRA[1, 2], Tiago SILVEIRA[1, 2],
Daniel FONSECA[1, 2], Rogério N. NOGUEIRA[1, 2], Paulo MONTEIRO[1, 2]

[1]Instituto de Telecomunicações, Campus Universitário de Santiago, 3810 Aveiro, Portugal

[2]Nokia Siemens Networks Portugal, 2720-093 Amadora, Portugal

*Corresponding author: mvd@av.it.pt

We present the optimization of an optical filtering module (OFM) of a single-channel 40 Gb/s transmission system with optical single-sideband modulation and alternate mark inversion signaling. Sideband suppression and dispersion compensation are simultaneously performed by the fiber Bragg grating (FBG) optical filtering through amplitude and phase response, respectively. Different amounts of accumulated dispersion are compensated using an OFM based on optical switches and chirped FBGs with different accumulated dispersion. Linear transmission simulations to assess the OFM effectiveness yield a Q-factor penalty variation lower than 1 dB relative to back-to-back considering a maximum accumulated dispersion of 20400 ps/nm. A transmission distance of 1040 km of nonlinear standard single mode fiber is achieved with a Q-factor higher than 7.

Keywords: optical single sideband (OSSB), alternate mark inversion (AMI), dispersion compensation (DC), fiber Bragg gratings (FBG).

1. Introduction

The growing volume and bandwidth demand of data services is leading to an increasing interest in ultradense wavelength division multiplexing (UDWDM) systems. The design of cost effective UDWDM systems greatly depends on the use of appropriate modulation formats. Such modulation formats enable high spectral efficiency, reduced signal degradation caused by interchannel crosstalk, and enhanced tolerance to fiber group velocity dispersion (GVD) [1]. Advanced modulation formats such as differential quadrature phase shift keying (DQPSK) [2], duobinary [1] or vestigial sideband [3] have been thoroughly investigated for use in such systems.

Optical single-sideband (OSSB) modulation has been proposed as a good candidate for implementation in such systems [4]. The sideband suppression can be achieved using one of two techniques: a phase-shift technique [4], or the use of a detuned optical

filter (OF) [5]. In the first technique, sideband suppression is achieved by adding the information signal and the Hilbert transform of the information signal. The Hilbert transform is obtained using a quadrature filter. As ideal quadrature filters are extremely difficult to implement, the main problem of this technique is the design of a device that approximates the Hilbert transform and operates at high bit rates. In the second technique, sideband suppression is achieved through detuned optical filtering. This technique enables the use of high bit rates, as it requires a transmitter with simpler electrical circuitry. Nevertheless, it has limitations. The use of pure intensity-modulated (IM) signals with non-return-to-zero (NRZ) or return-to-zero (RZ) pulses, and limited amplitude decay of feasible OFs result in reduced sideband suppression or carrier tone filtering [6]. However, optical signals with poor spectral content around the carrier frequency allow overcoming such disadvantage [6]. Alternate mark inversion (AMI) signaling is a good candidate due to the poor spectral content near the optical carrier and because it can be detected with conventional direct detectors [5]. An OSSB system with AMI−RZ signaling presented remarkable tolerance to GVD and improved tolerance to polarization mode dispersion relative to duobinary sideband in [5]. Moreover, OSSB−AMI−RZ systems with detuned optical filtering require simpler transmitter and receiver than DQPSK systems [2].

Dispersion compensation (DC) is an important issue in high per-channel bit rate systems. In optically routed networks, optical signals travel along different paths. As each path has its own dispersion profile, the signal at the receiver may have different values of accumulated dispersion on a short time scale. Therefore, the use of fast adaptable DC devices is imperative. The combination of such devices with proper dispersion maps results in better performance. Chirped FBGs can be used to perform DC. In comparison to dispersion compensating fiber (DCF), CFBGs have lower losses and insignificant nonlinear effects.

In this paper, the optimization of the optical filter module (OFM) of a 40 Gb/s OSSB−AMI−RZ single-channel system is presented. Sideband suppression is obtained by detuned filtering implemented by FBGs. The filter phase response is used to perform DC. The presented system is similar to that given in [5]. However, in [5] the filters are based on flat-top arrayed waveguide gratings (AWGs) and the DC is achieved with DCFs and periodic dispersion maps.

The remainder of this paper is structured as follows. Section 2 presents the description of the system setup and simulation parameters. In Section 3, the design of the FBGs used in the system is described. Optimization of the filter parameters is described in Section 4. Section 5 presents the linear and nonlinear transmission results. Section 6 presents a test of the system DC scheme robustness. Section 7 states the main conclusions of this work.

2. Setup description

A scheme of the system is shown in Fig. 1. The system is divided into three parts: a transmitter (TX), a transmission link (TL) and a receiver (RX). The modulation of
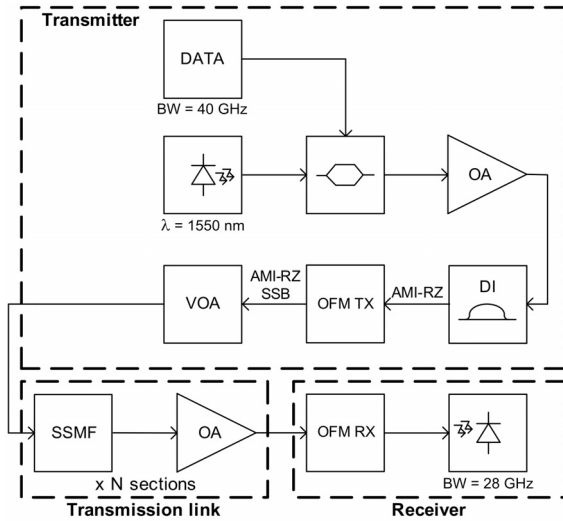
Fig. 1. OSSB system setup.

the AMI−RZ optical signal is performed with a Mach−Zehnder modulator (MZM) and a delay interferometer, as described in [7]. The deBruijn sequences with 2^{12} symbols are used to generate the data pattern. The frequency response of the TX electrical circuitry is modeled by a third-order Bessel filter with a −3-dB cutoff frequency equal to the bitrate. The optical source is an ideal continuous wavelength laser with an average power of 10 dBm. The MZM has insertion losses of 6 dB. The optical PSK signal at the output of the MZM is amplified by an optical amplifier (OA) that retrieves an average power of 18 dBm at its output. All the OAs of the system have a noise figure of 6 dB. A delay of 12.5 ps is used in the delay interferometer (DI) in order to obtain RZ pulses with a duty-cycle of 50%. The OFM TX performs sideband suppression and DC. The variable optical attenuator (VOA) sets the defined optimum power at the input of the TL.

The TL consists of one or more 80 km standard single mode fiber (SSMF) sections, interleaved with OAs. The SSMF has a dispersion parameter of 17 ps/nm/km, dispersion slope of 80 fs/(nm^{2}km), nonlinearity coefficient of 1.32 W^{-1}km^{-1} and attenuation coefficient of 0.2 dB/km. The OAs fully compensate the losses associated to one fiber section.

At the RX, a second OFM is used to compensate the remaining accumulated dispersion and perform noise filtering. The electrical part of the receiver is composed of an ideal square-law detector and an electrical filter modeled by a third-order Bessel filter with a −3-dB cutoff frequency of 28 GHz.

Figure 2 presents the OFM setup. Each device is composed by a five-port circulator, three optical switches (OSs) and respective FBGs. The OSs select the operating FBGs, depending on the TL length. The OFM is divided into three stages. The first stage is performed by a 1×6 OS and respective FBGs, used to compensate the accumulated dispersion of zero to five SSMF sections. If more accumulated dispersion needs to be compensated, the second stage is used. This stage is performed
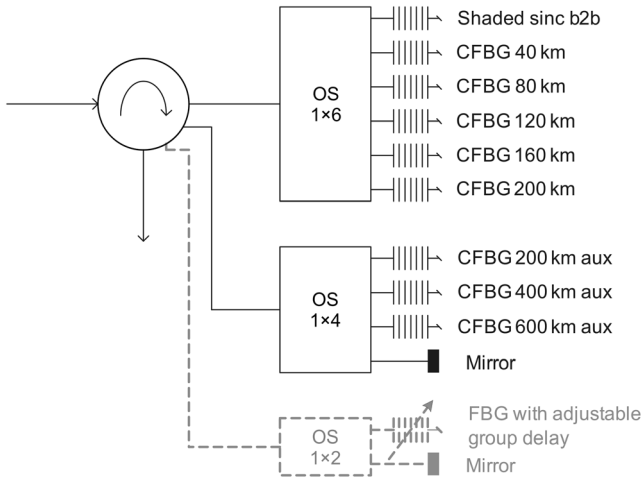
Fig. 2. OFM scheme (b2b – back-to-back). Each CFBG compensates the accumulated dispersion of the correspondent SSMF length.

by the 1×4 OS and respective FBGs. With these two stages an accumulated dispersion of zero to ten sections can be compensated. The third stage is composed of a 1×2 OS and a FBG with continuously adjustable group delay slope, as can be found in [8]. This stage can be used to provide continuous tunability to the OFM. The mirrors presented in Fig. 2 are used when the second and/or third stages are not needed. In this paper, only the first two stages are considered, since continuous dispersion compensation is not required. Although only one stage could be considered, this would result in having many FBGs. On the other hand, too many stages would result in high insertion losses due to the need of cascading several FBGs. Hence, employing three stages balances such drawbacks.

In order to achieve maximum number of sections with DC performed solely by the OFMs, each one compensates the same amount of accumulated dispersion, which is half the total accumulated dispersion. Consequently, the accumulated dispersion of twenty SSMF sections can be compensated. However, in this work, only zero to fifteen sections are considered. The choice of this dispersion map is discussed in Section 6.

3. FBG design

Second-order super-Gaussian filters are commonly used in optical systems. Although such filters are frequently implemented using AWGs, we use FBGs instead, due to the simplicity of implementation and the possibility of having sideband suppression and DC done in a single filter. Moreover, the design of FBGs with similar amplitude response and different DC values can be easily accomplished. The transfer function of the FBGs was obtained using the transfer matrix method [9].

As mentioned in Fig. 2, two different kinds of FBGs are considered: shaded--sinc [10], for transmission distances lower than 80 km; and linearly CFBGs [11] with
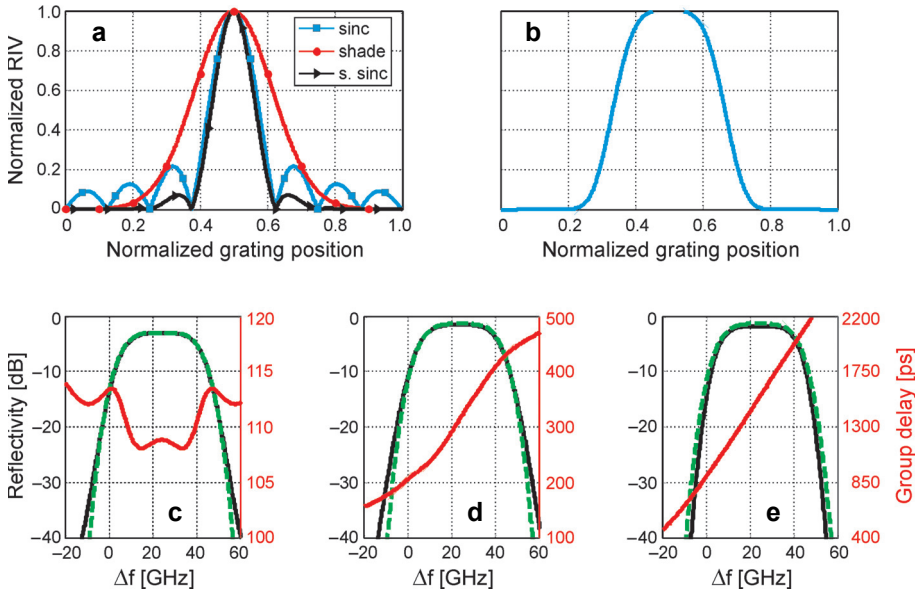
Fig. 3. Normalized refractive index profile of shaded sinc (**a**) and Gaussian apodizations (**b**); and frequency response of shaded sinc (**c**), CFBG 80 km (**d**); and CBFG 200 km (**e**). In graphics (**c**), (**d**) and (**e**), the dashed curve is the amplitude response of an ideal super-Gaussian filter. RIV – refraction index variation.

Gaussian apodization. These kinds of gratings differ in the apodization profile, as depicted in Figs. 3**a** and 3**b**. Fourier theory is applicable to grating responses when weak gratings (with reflectivity of approximately or less than 50%) are considered. Therefore, a sinc-shaped refractive index profile should result in a square overall reflection spectrum. Gratings with this refractive index profile have also proven to be almost dispersion free. The apodization of this profile with a Gaussian function (also called shading function) allows the control of the filter order without degrading significantly the group delay response (Fig. 3**c**). To obtain a second order super--Gaussian filter, a Gaussian shading function with a full width at half maximum (FWHM) of $L/3.7$ [9] is considered, where L is the grating length. Linearly CFBGs are useful for DC. To obtain a second-order super-Gaussian response, a second-order Gaussian profile with FWHM = $L/3$ is considered for all CFBGs. The adjustment of the refraction index, chirp and length of the grating allows changing the filter's dispersion without altering significantly the amplitude response (Figs. 3**d** and 3**e**).

The losses associated to optical filtering in the TX and RX OFMs are less than 7 and 5 dB, respectively. The FBGs maximum group delay ripple is 10 ps.

4. SSB filter optimization

In this section, the performance criteria and TX filter optimization are presented. In a first approach, the TX and RX OFM filtering is replaced by a single filter with

a second-order super-Gaussian response, as such filters can be implemented with FBGs.

Three different performance criteria are considered: –20 dB signal spectral bandwidth (SBW); Q-factor penalty (ΔQ) and sideband suppression ratio (SSR). The –20 dB SBW measurements are accomplished by finding the lowest spectral range with 99% of the total power of the optical signal. The Q-factor penalty in decibels is given by

$$\Delta Q = 20\log_{10}(Q_{ref}) - 20\log_{10}(Q_{OSSB}) \tag{1}$$

where Q_{OSSB} and Q_{ref} are the Q-factor of the OSSB and reference signals, respectively. The reference signal is an unfiltered NRZ signal with an extinction ratio (ER) of 10 dB, as considered in [12] for 40-Gb/s signals long-haul transmission. A semi-analytical approach is employed to estimate Q-factor, where the signal waveform is obtained using a numerical simulation, while the impact of optical noise is taken into account analytically [13]. The SSR in decibels is

$$SSR = 10\log_{10}(P_{NSSB}) - 10\log_{10}(P_{SSB}) \tag{2}$$

where P_{NSSB} and P_{SSB} are the optical powers of the non-suppressed and suppressed sidebands, respectively. A signal with SSR less than 20 dB is considered vestigial sideband, otherwise, it is considered SSB. The –20 dB SBW and SSR are measured at the TX OF output.

The filter optimization has two main purposes: improving the robustness to fiber dispersion and compacting the signal spectra [5]. Hence, the following criteria are used to select the filter settings: *i*) the –20 dB SBW is minimized; *ii*) ΔQ is minimized, and *iii*) the SSR is higher than 20 dB. Although the criteria chosen are similar to the ones used in [5], the optimum filter settings obtained in that work cannot be used in the system presented, as the AMI–RZ signal at the TX OF input has a duty cycle of 50%.

The optimization of the filter bandwidth and detuning is performed in back-to--back, according to the scheme presented in Fig. 4. The bandwidth of the RX OF should be high enough to enable reduced signal degradation and low enough in order to have efficient noise filtering. Therefore, a bandwidth of 40 GHz is chosen. The RX OF has equal detuning to the TX OF. At the RX OF output, an optical signal-to-noise ratio (OSNR) of 22.0 dB is considered. This value remains constant in all tests along
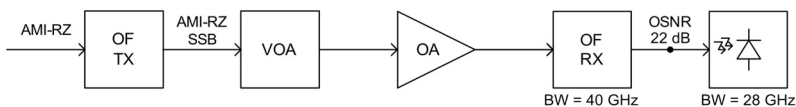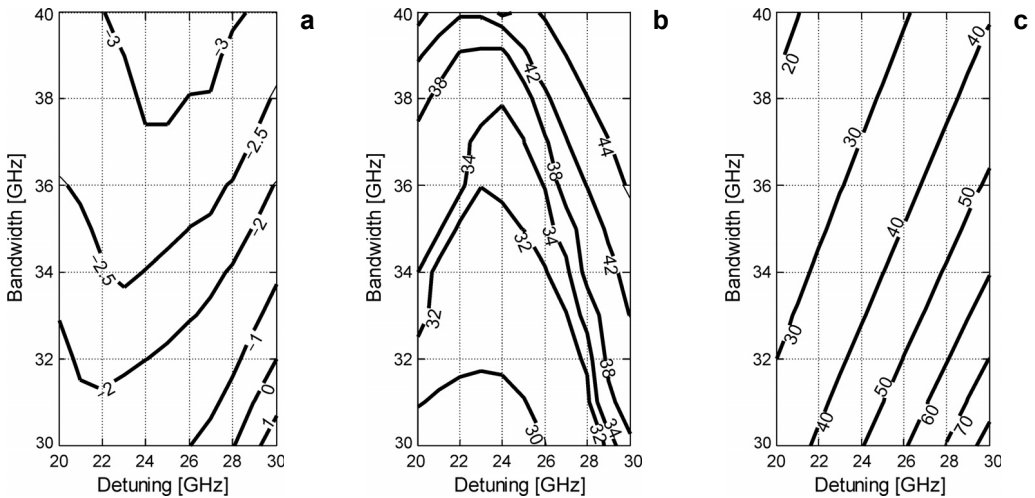

Fig. 4. TX OF optimization scheme.

Fig. 5. *Q*-factor penalty (**a**), −20 dB SBW (**b**), and SSR (**c**) for the TX OF bandwidths and detunings considered.

this section, and results in a *Q*-factor of 7 when the reference signal is used. The optimization results are presented in Fig. 5. Following the performance criteria described, a detuning of 24 GHz and a bandwidth of 35 GHz are considered. With these parameters, a filtered signal with a −2.7 dB of *Q*-factor penalty, 31.6 GHz of −20 dB SBW and 34.3 dB of SSR is obtained. Therefore, all FBGs were designed with a detuning of 24 GHz. The FBGs of the first stages of the TX and RX OFMs have a bandwidth of 35 and 40 GHz, respectively. The FBGs of the second stages must have a larger bandwidth to avoid changing significantly the amplitude response of combined filtering of first and second stages. Hence, the FBGs of the second stages of the TX and RX OFMs have a bandwidth of 55 GHz.

5. Transmission simulations

After optimizing the TX and RX FBG settings each OFM, the DC effectiveness and system performance are assessed.

The DC effectiveness is assessed with a linear transmission simulation. The simulation scheme is similar to the one presented in Fig. 1. Linear lossless SSMF sections are considered and an OSNR of 22.0 dB is set at the RX OFM output, independently of the number of sections. Figure 6 presents Δ*Q* as a function of the fiber length. The *Q*-factor penalty variation to the back-to-back case is lower than 1 dB, proving that the effectiveness of the optical DC does not change significantly with the fiber length considered.

The nonlinear transmission simulation scheme is the one presented in Fig. 1. The *Q*-factor as a function of the input power per section is presented in Fig. 7,
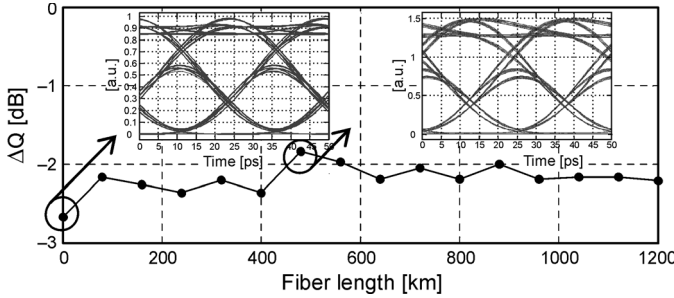
Fig. 6. *Q*-factor penalty for the linear transmission simulation. Inset: eye patterns for 0 and 480 km of linear SSMF.
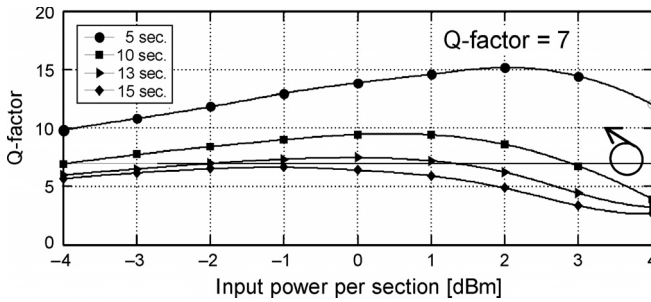

Fig. 7. *Q*-factor as a function of the input power per section.

considering different number of sections. Figure 7 shows that thirteen sections of SSMF are achieved with a *Q*-factor higher than 7, proving that the signal degradation arises mainly from the noise accumulation and fiber nonlinear effects.

6. Dispersion compensation robustness

In this section, we investigate the robustness of the system to different dispersion maps and small deviations in the DC. Thirteen sections and optimum input power per section (0 dBm) are considered. Both OFMs compensate half of the total accumulated
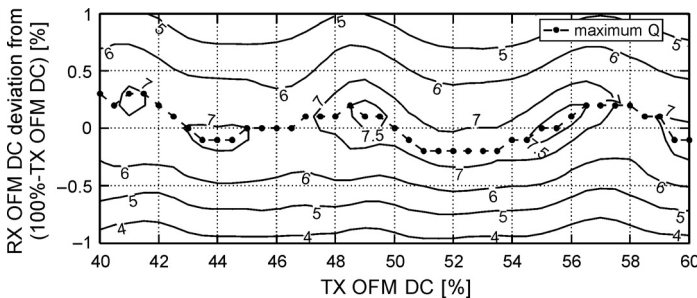

Fig. 8. *Q*-factor as a function of dispersion map and RX OFM DC deviation.

dispersion. The dispersion variation is performed by two linear lossless fiber sections, each one placed after the TX and RX OFMs. Figure 8 presents the *Q*-factor as a function of the total DC performed at the TX and deviation of the DC performed at the RX from the remaining DC. Considering optimum DC, a *Q*-factor variation of 1.2 dB is obtained for the dispersion maps considered, proving that the use of different dispersion maps results in negligible penalties. However, DC variations from the optimum value (dotted line) result in higher penalties. This attests the need for small adjustments of the DC, enabled by the third stage of the OFMs.

7. Conclusions

A 40 Gb/s OSSB transmission system with AMI−RZ signaling format and optical DC has been investigated. Sideband suppression and DC are both performed by optical filtering, implemented with FBGs. A scheme based on FBG switching has been proposed to perform DC for different SSMF lengths. Linear transmission simulation yielded a *Q*-factor penalty variation to the back-to-back case lower than 1 dB considering a maximum transmission distance of 1200 km. Nonlinear transmission simulation achieved a *Q*-factor higher than 7 for 1040 km of SSMF using optimum input power in each fiber section. Simulations with different dispersion maps yielded a maximum *Q*-factor variation of 1.2 dB. The use of the DC scheme presented with equal DC at the TX and RX has proven to be almost ideal. Moreover, the system has proven to be robust to different dispersion maps. However, DC variations from the optimum value result in significant penalties, proving the need for small adjustments of the DC.

References

[1] WINZER P.J., ESSIAMBRE R.J., *Advanced optical modulation formats*, Proceedings of the IEEE **94**(5), 2006, pp. 952−985.
[2] GRIFFIN R.A., CARTER A.C., *Optical differential quadrature phase-shift key (oDQPSK) for high capacity optical transmission*, [In] *Optical Fiber Communication Conference and Exhibit, OFC 2002*, pp. 367−368.
[3] SU Y., MOLLER L., RYF R., CHONGJIN XIE, XIANG LIU, *Feasibility study of 0.8-b/s/Hz spectral efficiency at 160 Gb/s using phase-correlated RZ signals with vestigial sideband filtering*, IEEE Photonics Technology Letters **16**(5), 2004, pp. 1388−1390.
[4] FONSECA D., CARTAXO A.V.T., MONTEIRO P., *Optical single-sideband transmitter for various electrical signaling formats*, Journal of Lightwave Technology **24**(5), 2006, pp. 2059−2069.
[5] CHARRUA P.M.A., CARTAXO A.V.T., *Performance analysis of AMI-RZ single-sideband signals in 40 Gbit/s transmission systems*, IEE Proceedings – Optoelectronics **153**(3), 2006, pp. 109−118.
[6] FONSECA D., CARTAXO A., MONTEIRO P., *Comparison and optimisation of optical single sideband transmitters*, IET Optoelectronics **1**(2), 2007, pp. 82−90.

[7] WINZER P.J., GNAUCK A.H., RAYBON G., CHANDRASEKHAR S., SU Y., LEUTHOLD J., *40-Gb/s return-to-zero alternate-mark-inversion (RZ-AMI) transmission over 2000 km*, IEEE Photonics Technology Letters **15**(5), 2003, pp. 766–768.

[8] MATSUMOTO S., OHIRA T., TAKABAYASHI M., YOSHIARA K., SUGIHARA T., *Tunable dispersion equalizer with a divided thin-film heater for 40-Gb/s RZ transmissions*, IEEE Photonics Technology Letters **13**(8), 2001, pp. 827–829.

[9] ERDOGAN T., *Fiber grating spectra*, Journal of Lightwave Technology **15**(8), 1997, pp. 1277–1294.

[10] IBSEN M., DURKIN M.K., COLE M.J., LAMING R.I., *Optimised square passband fibre Bragg grating filter with in-band flat group delay response*, Electronics Letters **34**(8), 1998, pp. 800–802.

[11] JUNHEE KIM, JUNKYE BAE, YOUNG-GEUN HAN, SANG HYUCK KIM, JE-MYUNG JEONG, SANG BAE LEE, *Effectively tunable dispersion compensation based on chirped fiber Bragg gratings without central wavelength shift*, IEEE Photonics Technology Letters **16**(3), 2004, pp. 849–851.

[12] *International Telecommunication Union (ITU-T) Recommendation G.959.1, Optical Transport Network Physical Layer Interfaces*.

[13] REBOLA J.L., CARTAXO A.V.T., *Gaussian approach for performance evaluation of optically preamplified receivers with arbitrary optical and electrical filters*, IEE Proceedings – Optoelectronics **148**(3), 2001, pp. 135–142.